Met. Mater. Int., Vol. 20, No. 1 (2014), pp. 99~103
doi: 10.1007/s12540-013-6008-9

Suppression of Discontinuous Precipitation in AZ91 by Addition of Sn

I. C. Jung[1], Y. K. Kim[1], T. H. Cho[1], S. H. Oh[1], T. E. Kim[1], S. W. Shon[1], W. T. Kim[2], and D. H. Kim[1,*]

[1]Yonsei University, Department of Metallurgical Engineering, 134 Shinchon-dong, Seodaemun-gu, Seoul 120-749, Korea
[2]Cheongju University, Applied Science Division, Naedeok-dong, Sangdang-gu, Cheongju, Chungbuk 360-764, Korea

(received date: 27 September 2012 / accepted date: 1 April 2013)

The effect of Sn (5 wt%) addition on the aging behavior of the AZ91 alloy has been investigated in the present study. The addition of Sn effectively suppresses the discontinuous precipitation during aging treatment. The aging response of the Sn containing AZ91 alloy is far better than that of the AZ91 alloy due to much higher density of continuous precipitation in the matrix. The yield strength and total elongation to failure at the peak aged condition of the AZ91 and Sn containing AZ91 alloys are 119.4 and 161.9 MPa and 8.8 and 8.6%, respectively, indicating that 35.6% increase of yield strength can be obtained by the addition of Sn in the AZ91 alloy maintaining almost same level of ductility.

Key words: alloy, solidification, aging, phase transformation, mechanical properties

1. INTRODUCTION

Recently, magnesium alloys receive a great attention as one of the important light weight alloys. In particular, cast magnesium alloys have potential to be used as cast parts in light weight vehicles replacing aluminum alloys due to their high specific strength and good castability [1,2]. However, the number of alloy systems for casting is very limited because of inferior mechanical and corrosion properties when compared to those for aluminum alloys. In general, Mg-Al system is the most widely used alloy for casting. Among the Mg-Al based alloys, AZ and AM are two major alloy series which are currently being used in light weight vehicles in the automotive industry. Among the alloys from both series, AZ91 (Mg-9Al-0.8Zn-0.2Mn, in wt%) offers a good combination of mechanical properties, corrosion resistance and castability [3,4].

The maximum solid solubility of Al in pure Mg is ~12.7 wt% at 437 °C and decreases to ~2.0 wt% at room temperature [5]. Therefore, addition of 9 wt% Al in Mg can result in the formation of large volume fraction of $Mg_{17}Al_{12}$ (β) precipitates during aging treatment, which eventually can improve the mechanical properties [6]. However, the precipitation of $Mg_{17}Al_{12}$ occurs in two different ways, i.e., discontinuous and continuous precipitation. Discontinuous precipitation occurs by the growth of an alternating lamellar structure of α-Mg and $Mg_{17}Al_{12}$ at high angle grain boundaries [7,8], and is known to be detrimental to the mechanical properties [9]. On the other hand, it is known that continuous precipitation of $Mg_{17}Al_{12}$ in the remaining α-Mg matrix is effective in enhancing the age hardening response [10]. Hence, effective suppression of the discontinuous precipitation is one of the key issues in improving the mechanical properties of AZ91 after age treatment. There have been several studies on the suppression of the discontinuous precipitation in AZ91 by minor addition of elements such as Au, Pb, Ca and rare earth (RE) elements [1,11-14]. By adding those elements, the discontinuous precipitation is significantly suppressed, and the microstructure after aging treatment is dominated by continuous precipitation. Hence, suppression of the dynamic discontinuous precipitation during high temperature exposure can improve the high temperature properties including the creep property. But, it has been reported that the hardness level after aging treatment decreases, or the kinetics for peak age hardening is slowed down by the addition of the minor elements. Minor addition of Sn has also been reported to be effective in suppressing the discontinuous precipitation in AZ91 [15]. Li *et al*. have shown that when 2 wt% of Sn is added in AZ91, no discontinuous precipitation can be observed after aging treatment [15]. But, again, the strength level of the Sn containing AZ91 is lower than AZ91. They speculated that it is due to the larger number of grains containing cellular discontinuous precipitation which can effectively hinder the dislocation movement in AZ91.

In the present study, Sn is selected as an alloying element

*Corresponding author: dohkim@yonsei.ac.kr

in AZ91. The addition of Sn will result in the formation of Mg_2Sn particles in the interdendritic region during solidification which may effectively suppress the discontinuous precipitation during aging treatment. At the same time, solute Sn atoms which remain in the matrix after the solution treatment may accelerate the continuous precipitation since Sn has a reasonably high solubility in Mg [5], and the atomic size between Mg and Sn is larger than that between Mg and Al [16]. The presence of solute Sn atoms in the matrix can induce the misfit strain, which may act as heterogeneous nucleation site of the precipitates [17]. We have added larger amount of Sn (5 wt%) in AZ91 to investigate how the addition of Sn affects both discontinuous and continuous precipitation phenomena. As a result, we found that the discontinuous precipitation is suppressed as reported before, but the strength level after aging treatment is enhanced significantly due to much more accelerated continuous precipitation of the β phase in the α-Mg matrix.

2. EXPERIMENTAL PROCEDURES

AZ91(Al: 8.7 wt%, Mn: 0.13 wt%, Zn: 0.7 wt%) and 5 wt% Sn containing AZ91 (will be referred to as AZT915 hereafter) were selected for investigation in the present study. The alloy ingots were prepared in an electrical resistance furnace under a mixture of SF_6 and CO_2 protective gas atmosphere using high purity metals. When the temperature reached 1023 K, Sn was added into the melt to prepare the AZT915 alloy ingot. The melt was retained at 973 K for 30 min, and then was stirred to add a refining flux. Molten metal was poured into a preheated (~373 K) rectangular steel mold with a dimension of 1 cm in thickness, 6 cm in width, and 10 cm in height. The resulting alloys were solution treated at 683 K for 24 h, and then the samples were immediately water-quenched. After solid solution treatment, the cast ingot was cut into disks with a dimension of 10 mm in diameter and 4mm in thickness for the isothermal aging treatment. Artificial aging treatments were conducted at 441 K up to 28 h in an oil bath. The conditions for solution treatment and aging in the present study were selected following those in the ASTM Handbook [18]. Age-hardening response was investigated by using Vickers hardness measurements (MXT-ZX7E) under a load of 1 kg_f. Proper hardness value was obtained from at least five individual measurements. The specimens for optical microscopy (LEICA DMRM optical microscope) and scanning electron microscopy (JEOL™, JSM7001F) were prepared by etching with a solution of 4 ml nitric acid and 96 ml ethanol. Specimens for transmission electron microscopy (JEOL™, JEM2000EX) were prepared using an ion milling equipment (Gatan™, model 600) under the cooling condition by circulating liquid N_2. The microstructural examination was performed using a TEM operating at 200 kV.

For tensile property measurement the alloy ingots were prepared using a centrifugal casting method to minimize the effect of the impurities on the mechanical properties. The diameter and thickness of the mold was 280, and 10 mm, respectively. The rotating speed was 1000 rpm. The resulting ingots were machined to tensile test specimens with gauge length of 25 mm [19]. Tensile properties of the cast alloys were evaluated using universal testing machine (INSTRON5967) at a strain rate of 1×10^{-3} s^{-1}.

3. RESULTS AND DISCUSSION

Figures 1(a) and (b) show typical optical micrographs obtained from the as-cast AZ91 and AZT915 alloys. Both the as-cast microstructure consisted of α-Mg dendrite and secondary solidification phases in the interdendritic region. As reported previously [20,21], a eutectic structure consisted of α-Mg and β was found in the interdendritic region of AZ91. In addition, Mg_2Sn was present in the interdendritic region of AZT915. The presence of Mg_2Sn can be clearly identified in the solution treated sample shown in Fig. 1(d). In the case of AZ91 (Fig. 1(c)), the β phase is completely dissolved into the matrix. However, in the case of AZT915, Mg_2Sn remains in the matrix due to its higher melting temperature.

The microstructural development during aging treatment at 441 K has been investigated using OM and SEM. Figs. 2(a) and (b) show optical micrographs obtained from the AZ91 and AZT915 alloys after aging for 16 h. The regions with darker contrast at the grain boundaries in the optical micrographs represent the area where the discontinuous precipitation occurred during aging treatment. In general, the grain boundaries are outlined more clearly than those in the solution treated sample (Figs. 1(c) and (d)) due to the discontinuous precipitation at the grain boundaries. Comparison of the optical micrographs in Figs. 2(a) and (b) clearly reveals

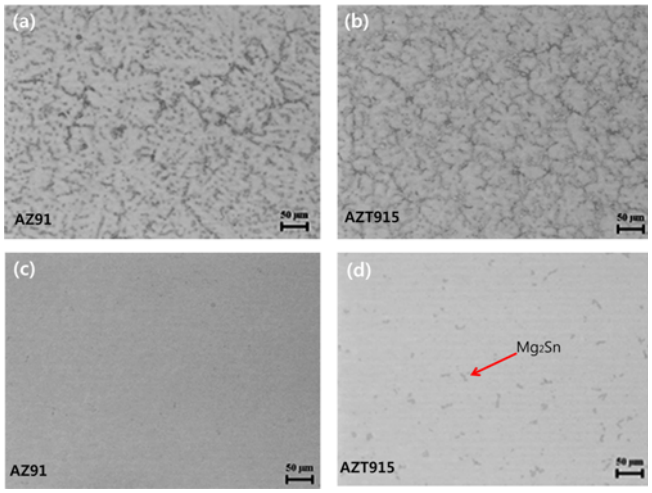

Fig. 1. Optical micrographs obtained from: as-cast (a) AZ91; and (b) AZT915: and solution treated (c) AZ91, and (d) AZT915.

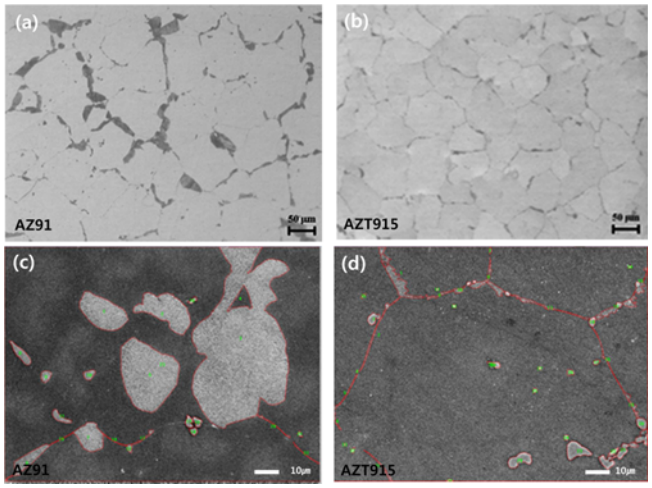

Fig. 2. Optical micrographs obtained from: (a) AZ91, and (b) AZT915 after aging at 441 K for 16 h, secondary electron micrographs obtained from, (c) AZ91, and (d) AZT915 after aging at 441 K for 16 h.

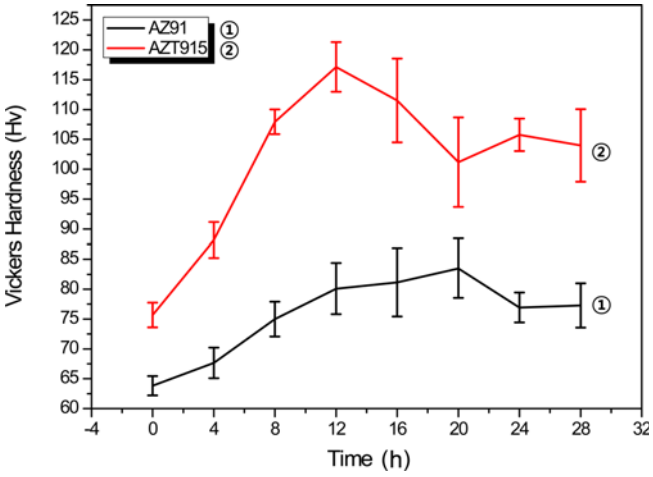

Fig. 3. Hardness variation during aging treatment of AZ91 and AZT915 at 441 K.

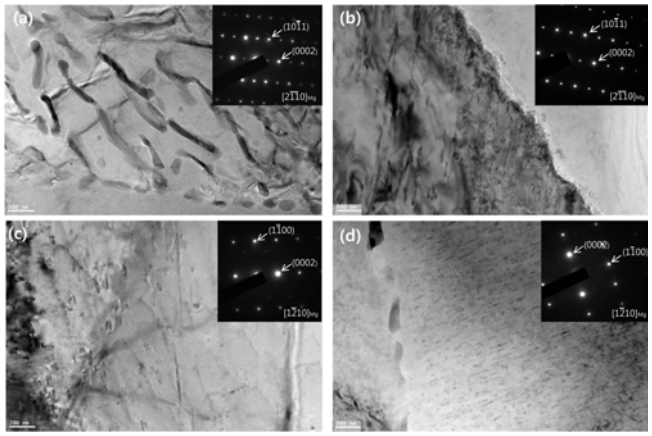

Fig. 4. Bright TEM images obtained from: (a) AZ91, and (b) AZT915 after aging at 441 K for 5 h, (c) AZ91, and (d) AZT915 after aging at 441 K for 16 h. The corresponding selected area diffractions are inserted in the micrographs.

that the discontinuous precipitation at the grain boundaries is significantly suppressed by addition of Sn, as reported previously [15]. The SEM micrographs in Figs. 2(c) and (d) obtained from the AZ91 and AZT915 alloys after aging for 16 h show the lamellar structure of the discontinuous precipitation. From the SEM micrographs, the volume fraction of the discontinuous precipitation was evaluated to be 26.8% in AZ91, and 4.0% in AZT915 using an image analyzer. The progress of the discontinuous precipitation depends on several parameters, for example aging temperature, grain size and solute supersaturation in the matrix [22]. Generally, it is known that the rate for the nucleation of the discontinuous precipitation in Mg-9Al based alloys is inversely proportional to the unit square of the average grain size [23-25]. However, the grin size was similar after the aging treatment, as can be seen in Figs. 2(a) and (b). Li et al showed that the discontinuous precipitation disappears completely when 2 wt% Sn is added [15]. On the contrary, in the present study, 4.0% of the discontinuous precipitation remains after the aging treatment. The difference may come from the different heat treatment conditions, however, the detailed study is required to reveal the effect of the added amount of Sn.

The variation of hardness during aging treatment of AZ91 and AZT915 alloys at 441 K is shown in Fig. 3. It can be noticed that a significant increase of hardness occurs with the addition of Sn in AZ91. The hardness before starting the aging treatment, i.e. after the solution treatment in AZT 915 (Hv 75.68) is higher than that in AZ91 (Hv 63.82), which is thought to be due to the particle strengthening effect by the Mg_2Sn particles at the grain boundary and solid solution strengthening effect by the Sn solute in the matrix. In AZT915, the hardness increases steeply with the start of the aging treatment, reaching the peak hardness value of Hv 117.14 after aging for 12 h. On the contrary, AZ91 shows a less steep increase of hardness, exhibiting the highest value of hardness (Hv 83.48) after 20 h aging treatment. Such a significant increase of hardness with the addition of 5 wt% Sn is interesting, since in the previous studies it has been shown that with the addition of minor element such as Pb, Ca Au and RE elements the hardening kinetics is delayed or the peak hardness value is decreased, although the occurrence of the discontinuous precipitation is suppressed [1,11,12]. To reveal the possible reasons for such an enhancement of hardness, the microstructural evolution with aging treatment was investigated using TEM. Figs. 4(a) and (b) show typical bright field TEM images obtained from the AZ91 and AZT915 alloys after aging at 441 K for 5 h. The inserted selected area diffraction pattern indicates that the α-Mg matrix in Figs. 4(a) and (b) is oriented along the same zone axis of $[01\bar{1}0]$

zone axis of the hcp structure. In AZ91, the discontinuous precipitation progressed to a large extent even after 5 h aging treatment. On the contrary, the evidence of the discontinuous precipitation is rarely found in AZT915, implying that the addition of Sn significantly suppress the discontinuous precipitation. It is considered that the Mg_2Sn phase particles at the grain boundary effectively reduces the possible nucleation sites for the β precipitates, and slow down the movement of the grain boundary which is required for the formation of the discontinuous precipitation. Figs. 4(c) and (d) show typical bright TEM images obtained from the AZ91 and AZT915 alloys after aging at 441 K for 16 h. The inserted selected area diffraction pattern indicates that the α-Mg matrix in Figs. 4(c) and (d) is oriented along the same zone axis of [11$\bar{2}$0] of the hcp structure. Figs. 4(c) and (d) particularly compare the density of the continuous precipitation in the matrix. It can be noticed that much higher density of continuous precipitation occurred in the AZT915 alloy than in the AZ91 alloy. In AZ91, depletion of Al due to the formation of discontinuous precipitates may lead to much less density of continuous precipitates. On the contrary, in AZT915, the presence of Sn solute in the matrix may lead to the enhanced nucleation rate of the precipitates. Li *et al*. have shown that 2 wt% Sn addition in AZ91 results in the decrease of the strength level after aging treatment [15]. Therefore, it can be inferred that the addition of 2 wt% Sn is not enough to lead such a copious nucleation of the β precipitates in the matrix. The results in the present study indicate that the enhancement of the nucleation rate of the precipitates in the matrix by adding a proper amount of elements such as Sn is very important to enhance the aging response of the AZ91 alloy. The reason for the less eminent aging response in the previous studies [1,12,15] in spite of the effective suppression of the discontinuous precipitation is thought to be the less activated continuous precipitation process in the matrix.

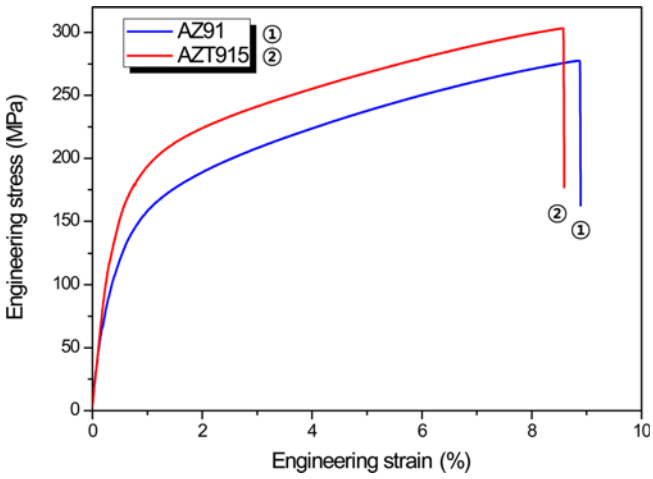

Fig. 5. Stress-strain curves obtained from AZ91 and AZT915 aged at 441 K for 20 and 12 h, respectively.

Table 1. The tensile test results of AZ91 and AZT915 aged at 441K

Alloys	T6 condition		Y.S (MPa)	U.T.S (MPa)	Elongation (%)
	Holding Temperature (K)	Holding Time (h)			
AZ91	441	20	119.4	277.5	8.8
AZT915	441	12	161.9	303.4	8.6

Figure 5 shows the stress-strain curves obtained from the AZ91 and AZT915 alloys aged at 441 K for 20 and 12 h, respectively. The AZT915 alloy at the peak aged condition shows far better tensile properties than the AZ91 alloy, as shown in Table 2. In particular, the yield strength increased from 119.4 MPa to 161.9 MPa, i.e. by 35.6%, while maintaining almost same level of ductility. The improvement of the strength level is due to the precipitation of high-density fine β phase in the matrix and the suppression of the discontinuous precipitation at the grain boundaries.

4. CONCLUSIONS

(1) The addition of Sn effectively suppresses the discontinuous precipitation in AZ91. The volume fraction of the discontinuous precipitation in AZ91 and AZT915 is 26.8 and 4.0%, respectively after aging at 441 K for 16 h.

(2) Aging response of AZT915 is far better than that of AZ91. The hardness increases steeply with the start of the aging treatment, reaching the peak hardness value of Hv 117.14 after aging for 12 h in AZT915, while the hardness increases less steeply reaching peak hardness value of Hv 83.48 after aging for 20 h in AZ91.

(3) Better aging response in AZT915 is due to the much higher density of continuous precipitation. The significant increase of the density of the precipitates in AZT915 is due to the enhanced nucleation rate of the continuous precipitates by the presence of Sn solute in the matrix.

(4) The yield strength and total elongation to failure at the peak aged condition of AZ91 and AZT915 are 119.4 and 161.9 MPa and 8.8 and 8.6%, respectively, indicating that 35.6% increase of yield strength can be obtained by the addition of Sn in AZ91 maintaining almost same level of ductility.

ACKNOWLEDGMENTS

This study was supported by the World Premier Materials (WPM) project funded by the Korea Ministry of Knowledge and Economy, and the Global Research Laboratory Program of Korea Ministry of Education, Science and Technology.

REFERENCES

1. A. Srinivasan, U. T. S. Pillai, and B. C. Pai, *Mater. Sci. Eng. A* **452-453**, 87 (2007).

2. S. S. Park, Y. S. Park, and N. J. Kim, *Met. Mater. Int*. **8**, 551 (2002).
3. D. Wenwen, S. Yangshan, and W. Dengym, *Mater. Sci. Eng. A* **356**, 1 (2003).
4. Y. Guangyin, S. Yangshan, and D. Wenjiang, *Mater. Sci. Eng. A* **308**, 38 (2001).
5. A. A. Nayeb-Hashemi and J. B. Clark, *ASM International* (1998).
6. J. B. Clark, *Acta Metall*. **16**, 141 (1968).
7. I. Manna, S. K. Pabi, and W. Gust, *Int. Mater. Rev.* **46** 53 (2001).
8. D. Duly, J. P. Simon, and Y. Brechet, *Acta Metall. Mater.* **43** 101 (1994).
9. Q. Wang, W. Chen, W. Ding, Y. Zhu, and M. Mabchi, *Metall. Mater. Trans. A* **32**, 787 (2001).
10. D. Duly, M. C. Cheynet, and Y. Brechet, *Acta Metall*. **42**, 3843 (1994).
11. B. A. Esgandari, H. Mehjoo, B. Nami, and S. M. Miresmaelil, *Mater. Sci. Eng. A* **528**, 5018 (2011).
12. C. J. Bettles, *Mater. Sci. Eng. A* **348,** 280 (2003).
13. K. T. Kashyap, C. Ramachandra, M. Sujatha, and B. Chatterji, *Bull. Mater. Sci*. **23**, 39 (2000).
14. N. Balasubramani, A. Srinivasan, U. T. S. Pillai, and B. C. Pai, *Mater. Sci. Eng. A* **457**, 275 (2007).
15. R. G. Li, Y. Xu, W. Qi, J. An, Y. Lu, W. Y. Cao, and Y. B. Liu, *Mater. Charact.* **59**, 1643 (2008).
16. E. Clementi and D. L. Raimondi, *J. Chem. Phys*. **38**, 2686 (1963).
17. K. N. Braszczyńska-malik. *J. Alloys Compd*. **477**, 870 (2009).
18. M. M. Avedesian and H. Baker, *ASM Specialty Handbook*, pp.78-84, ASM International, USA (1999).
19. ASTM, ASTM E8 Standard Test Methods for Tension Testing of Metallic, http://www.astm.org (2012).
20. Z. Zhao, Q. Chen, Y. Wang, and D. Shu, *Mater. Sci. Eng. A* **515**, 151 (2009).
21. C. D. Lee, *Met. Mater. Int*. **8**, 283 (2002).
22. A. Srinivasan, U. T. S. Pillai, and B. C. Pai. *Mater. Sci. Eng. A* **527**, 6543 (2010).
23. D. Duly, J. P. Simon, and Y. Brechet. *Acta Metall*. **43**, 101 (1995).
24. D. Bradai, P. Zieba, E. Bischoff, and W. Gust, *Mater. Chem. Phys*. **78**, 222 (2002).
25. S. H. Kim, B. H. Kim, K. C. Park, Y. H. Park and I. M. Park, *Korean J. Met. Mater.* **50**, 711 (2012).